

# Spin Transitions in Fe(II) Metallogrids Modulated by Substituents, Counteranions, and Solvents

Yi-Tong Wang, Shu-Tao Li, Shu-Qi Wu, Ai-Li Cui, De-Zhong Shen, and Hui-Zhong Kou\*

Department of Chemistry, Tsinghua University, Beijing 100084, P. R. China

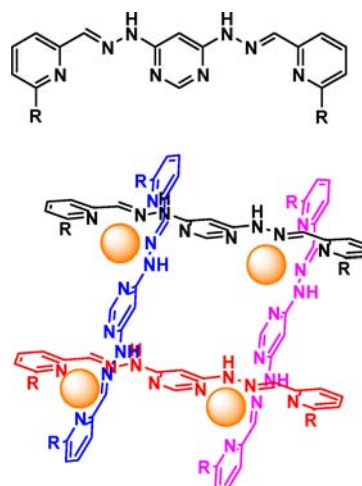
**S** Supporting Information

**ABSTRACT:** Two bis(tridentate) Schiff base ligands  $H_2L^x$  were used to construct three  $2 \times 2$  grid-type tetranuclear Fe(II) complexes 1–3 to obtain polynuclear spin-crossover materials. Magnetic susceptibility measurements show that the spin states of the complexes are related to the substituents of  $H_2L^x$ , and that spin transition occurs only in complexes 1 and 2, which are derived from a bulky ligand, whereas complex 3 is diamagnetic. The transition temperatures of complexes 1 and 2 are close to room temperature and are dependent on counteranions. The spin transition of complex 1 can be reversibly tuned by the dehydration and hydration process.

Switchability at the molecular level is an interesting property in chemistry.<sup>1,2</sup> The spin-crossover (SCO) between a high-spin (HS) state and a low-spin (LS) state is a promising way of attaining bistability or even multistability, thereby increasing the efficiency of information storage materials.<sup>3–7</sup> Most of the vast number of SCO complexes are mononuclear, Fe(II)-centered complexes<sup>8–11</sup> that provide useful experimental information to allow research to be rationally extended to polynuclear complexes. Factors such as the ligand field, counterions, and crystallization solvents are of vital importance in SCO studies.<sup>12–15</sup> Supramolecular strategies have been employed to generate an ordered assembly of metal ions, whereby both ligands and metal ions and even polynuclear molecules are self-assembled in a regular way.<sup>16–19</sup> Grid-like complexes are well-designed models that arrange from the  $2 \times 2$  to the  $n \times n$  level ( $n = 3, 4, \dots$ ) and display fascinating physical properties and aesthetically appealing structures.<sup>5,6,16–30</sup> However, to date, few grid-like SCO complexes have been created,<sup>5,6,17,26–30</sup> and the relationships between the metal ions within a grid and between the grids in a lattice are still not clear. SCO phenomena usually take place at low temperatures ranging from 100 to 250 K,<sup>31</sup> and thus it is always a challenge in practical applications to attain a transition temperature around room temperature.<sup>27</sup>

We have recently reported the first family of  $2 \times 2$  grid-like Fe(III) complexes, which exhibit weak antiferromagnetic coupling between high-spin Fe(III) ions via pyrimidine bridges.<sup>32</sup> Here we describe three novel  $2 \times 2$  grid-like Fe(II) complexes,  $[Fe_4(HL^1)_4]Cl_4 \cdot 9H_2O$  (1),  $[Fe_4(L^1)_2(H_2L^1)_2](BF_4)_4 \cdot 6H_2O$  (2), and  $[Fe_4(L^2)_2(H_2L^2)_2](ClO_4)_4 \cdot 4H_2O$  (3), that are derived from new bis(tridentate) Schiff base ligands  $H_2L^x$  (Scheme 1). Complexes 1 and 2 exhibit abrupt SCO at temperatures higher than room temperature, and complex 1

**Scheme 1.** Structure of  $H_2L^1$  (R = Br) and  $H_2L^2$  (R = Me) and  $[Fe_4(HL^x)]^{4+}$  Grids



shows a reversible spin switch following a repeated dehydration–hydration process. These results are significant for the practical application of such complexes as molecular storage devices.

Ligand  $H_2L^1$  was reacted with  $FeCl_2 \cdot 4H_2O$  in methanol at room temperature to give a solution. After filtration, the filtrate was slowly evaporated, producing dark red block crystals of complex 1 after 1 week. Single crystals of complexes 2 and 3 were obtained by the slow diffusion of an aqueous solution of  $NaBF_4/NaClO_4$  into a methanolic solution of  $FeCl_2 \cdot 4H_2O$  and  $H_2L^1/H_2L^2$  (Supporting Information). The mass spectrum of complex 1 in MeOH (Figure S1) showed peaks for species  $[Fe_4(HL^1)(L^1)_3]^+$  ( $m/z = 2120.46$ ),  $[Fe_4(HL^1)_2(L^1)_2]^{2+}$  ( $m/z = 1060.73$ ),  $[Fe_4(HL^1)_3(L^1)]^{3+}$  ( $m/z = 707.49$ ), and  $(H_2L^1+H)^+$  ( $m/z = 476.96$ ), indicating that tetranuclear Fe(II) grids are stable in solution. The formulas of complexes 1 and 2 were confirmed by microelemental analysis results and crystallography.

The molecular structures of complexes 1–3 were determined by single-crystal X-ray diffraction (XRD) analysis measured at ca. 150 K. The complexes have a similar  $2 \times 2$  grid  $[Fe_4]^{4+}$  structure composed of four ligands and four Fe(II) ions in an octahedral coordination geometry (Figure 1). Two ligands lie above the plane defined by the Fe(II) ions, and two lie below. Each of the four Fe(II) ions is coordinated by six nitrogen

Received: December 27, 2012

Published: April 2, 2013

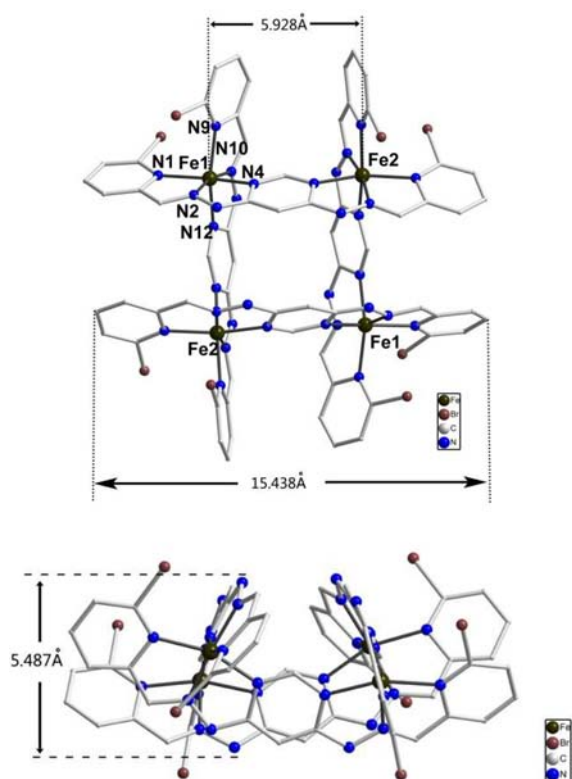


**Figure 1.** Molecular structure of the  $\text{Fe}_4$  cation in complex 1. The H atom, anions, and solvents are omitted for clarity.

atoms from two ligands (two pyrimidine N, two imine N, and two pyridine N atoms). The bond lengths of Fe–N in the complexes range from 1.88 to 2.06 Å, which is within the range of the LS Fe(II)–N bond lengths reported in mononuclear SCO complexes.<sup>1–3,15</sup> The average Fe–N bond distances are 1.971 Å for complex 1, 1.977 Å for complex 2, and 1.969 Å for complex 3. The adjacent Fe(II) ions are bridged by pyrimidine –N–C=N– bridges with an average Fe...Fe separation of 5.928 Å for complex 1, 6.063 Å for complex 2, and 6.053 Å for complex 3, and diagonal Fe...Fe distances within the grid of 8.291 Å for complex 1, 8.574 Å for complex 2, and 8.561 Å for complex 3.

The Fe(II) ions in a grid of complex 1 are not planar, whereas the grids of complexes 2 and 3 are more regular, with the four Fe(II) ions in a perfect plane (Figures S5 and S8). The conjugated ligands  $(\text{HL}^x)^- / (\text{L}^x)^{2-}$  are not planar but rather have a twisted pattern with the dihedral angles between the terminal pyridine planes in the range of 16.8–30.6°.

The octahedral distortion parameters ( $\Sigma$  and  $\Delta$ ),<sup>33,34</sup> Table 1) of complexes 1 and 2 are a little large, indicating the presence of a degree of distortion in the Fe(II) coordination geometry, which is consistent with mixed HS/LS states for the two complexes at 153 K. The smaller distortion parameters of

**Table 1.** Comparison of the Fe–N Bond Lengths (Å) and the Structural Distortion Parameters of Complexes 1–3

	Fe–N	Fe–N <sub>av</sub>	$\Sigma/^\circ$	$\Delta$
1	1.881(13)–2.036(13), 1.895(11)–2.064(13)	1.961(13), 1.981(13)	87.7	$1.78 \times 10^{-3}$
2	1.892(3)–2.058(3)	1.977(4)	85.7	$2.27 \times 10^{-3}$
3	1.882(4)–2.042(4)	1.969(4)	83.1	$1.04 \times 10^{-3}$

complex 3 are in good agreement with the LS state of all Fe(II) ions with an electronic configuration of  $t_{2g}^6$ . However, the dihedral angle  $\psi$  between the mean planes defined by the atoms of the two  $(\text{HL}^x)^- / (\text{L}^x)^{2-}$  ligands is close to 90°, implying the LS of Fe(II).<sup>35</sup>

The weak intermolecular Br... $\pi$  interactions in complex 1 connect the grids in a 3D network with water molecules and chloride ions incorporated within the formed cavities (Figures S3 and S4). The hydrogen-bonding interactions between the hydrazine groups of  $\text{H}_2\text{L}^x / (\text{L}^x)^{2-}$  of the adjacent grid molecules link the grid molecules of complexes 2 and 3 into a 1D network (Figures S6 and S9). In a direction perpendicular to the 1D chain, the adjacent grids are linked by C–H... $\pi$  interactions to form a 2D layer (Figures S7 and S10). The 1D chains and the 2D layers interlock, yielding a 3D open framework (Figure S11). The crystallization water molecules are regularly situated in the vicinity of the grids and form a 1D chain.

Magnetic susceptibility measurements reveal anion-, substituent-, and solvent-dependent magnetic behavior. It has been shown that the magnetic coupling through pyrimidine is weakly antiferromagnetic and negligible.<sup>32</sup> Thus, the complexes can be treated as independent Fe(II) centers connected by the ligands. For complexes 1 and 2, the  $\chi_m T$  shows an abrupt spin transition from LS state to HS state above 300 K, although this is incomplete (Figure 2). The magnetic susceptibility  $\chi_m T$  of

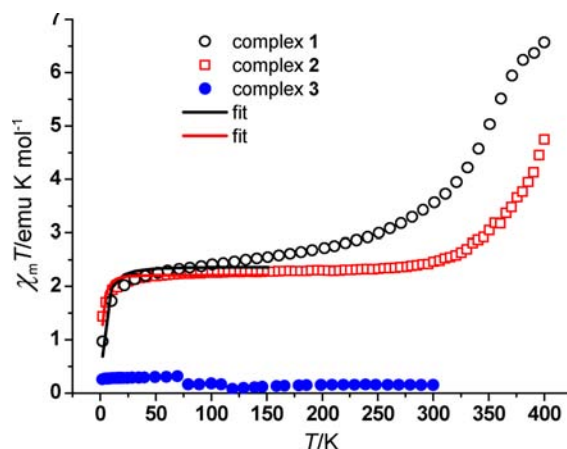


**Figure 2.** Plot of  $\chi_m T$  versus  $T$  for complexes 1–3. The solid lines represent the fitting results using the parameters discussed in the text.

complex 1 is 6.56  $\text{emu K mol}^{-1}$  per  $\text{Fe}_4$  at 400 K, decreasing to 2.41  $\text{emu K mol}^{-1}$  at 100 K as the temperature decreases. The  $\chi_m T$  value remains nearly constant until 30 K, and decreases further to 0.81  $\text{emu K mol}^{-1}$  at 2 K. As the expected spin-only  $\chi_m T$  value of the four HS Fe(II) ions is 12  $\text{emu K mol}^{-1}$ , the  $\chi_m T$  value of complex 1 at 400 K indicates that about 55% of the four Fe(II) ions are in the HS state. The  $\chi_m T$  plateau of 2.2  $\text{emu K mol}^{-1}$  suggests that 18% of the Fe(II) ions are in the HS state. A few Fe(II) complexes show the  $\chi_m T$  value of 2.0  $\text{emu K mol}^{-1}$  as an intermediate or stable spin state at low temperatures.<sup>36,37</sup>

The analogous phenomena are also displayed in complex 2, in which the spin transition starts at around 280 K. Complex 3, however, is diamagnetic at 300 K. These results imply that the methyl group is not sufficiently large to achieve a spin transition. This size effect can be rationally used to construct SCO complexes. The difference in the transition temperatures of complexes 1 and 2 is probably related to the difference in the

intermolecular interactions. The  $\text{Fe}_4$  grid analogues reported by Lehn et al. exhibit spin transition behavior when a bulky benzene group is introduced at the 2-position of the pyrimidine.<sup>28,30</sup> We show that the introduction of a bulky 6-bromo-substituted pyridine is an alternative means of generating spin transition in Fe(II) grid complexes.

The decrease in  $\chi_m T$  below 30 K should be due to the zero-field splitting (ZFS) effect of the remaining HS Fe(II) ( $S = 2$ ).<sup>30</sup> The data below 150 K were fitted by the equation derived from the Hamiltonian  $H = D[S_z^2 - S(S + 1)/3]$ , to give the ZFS parameters  $|D| = 7.7(10) \text{ cm}^{-1}$  for complex 1 and  $4.4(3) \text{ cm}^{-1}$  for complex 2 (solid lines in Figure 2).

Thermogravimetric analysis of complex 1 shows that the crystallization water of the complex is removed when heated to 400 K (experimental 6.6%, calculated 6.68%, Figure S12). Complex 1 loses nine lattice water molecules to become the dehydrated complex 1-9 $\text{H}_2\text{O}$  according to magnetic measurements performed up to 400 K. On cooling from 400 to 2 K, the dehydrated complex 1-9 $\text{H}_2\text{O}$  exhibits gradual SCO behavior that is distinct from that of the hydrated complex 1 (Figure 3).

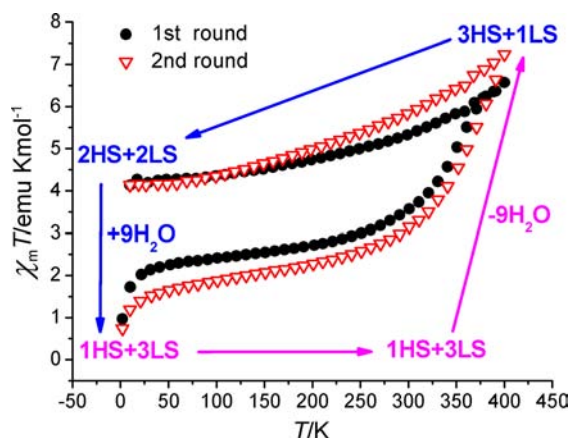


**Figure 3.** Temperature dependence of  $\chi_m T$  for the hydrated and dehydrated samples of complex 1. The number of Fe(II) with different spin states is assessed approximately.

The  $\chi_m T$  value of 1-9 $\text{H}_2\text{O}$  at 300 K is  $5.32 \text{ emu K mol}^{-1}$ , which is higher than that of complex 1 ( $3.57 \text{ emu K mol}^{-1}$ ). The  $\chi_m T$  value of complex 1-9 $\text{H}_2\text{O}$  at 20 K,  $4.27 \text{ emu K mol}^{-1}$ , approximately corresponds to the presence of two HS and two LS Fe(II) ions per  $\text{Fe}_4$  molecule. The distinct magnetic behavior of the hydrated complex 1 and the dehydrated complex 1-9 $\text{H}_2\text{O}$  is typical of the guest effect.<sup>14,15,36-40</sup>

Complex 2 loses six crystallization water molecules to become the dehydrated complex 2-6 $\text{H}_2\text{O}$  at 400 K (Figure S12). The dehydrated sample also displays magnetic behavior different from that of the hydrated sample: the  $\chi_m T$  versus  $T$  curve of the dehydrated complex 2-6 $\text{H}_2\text{O}$  is below that of the hydrated complex 2 across the whole temperature range (Figure S13). Complex 2-6 $\text{H}_2\text{O}$  has a  $\chi_m T$  value of  $2.96 \text{ emu K mol}^{-1}$  at 400 K, which is lower than that of complex 2,  $4.77 \text{ emu K mol}^{-1}$ . At 300 K, the  $\chi_m T$  values are 1.62 and  $2.39 \text{ emu K mol}^{-1}$  for complexes 2-6 $\text{H}_2\text{O}$  and 2, respectively. These results indicate that more Fe(II) ions are in the LS state after the removal of the crystallization water molecules, which is different from that in complex 1.

The reversibility of the magnetic behavior with dehydration-hydration was investigated. When the solid of complex 1-9 $\text{H}_2\text{O}$  was immersed in water at  $40^\circ\text{C}$  for 5 h, the obtained

sample became the hydrated complex 1, as verified by the powder XRD result (Figure S14) and microelemental analyses. The rehydrated sample was subjected to a new round of magnetic measurements. The magnetic susceptibility is consistent with the first-round data for complex 1 (Figure 3). The process is thus reversible by absorbing and losing crystallization water. In this case, removal of the crystallization solvent molecules of complex 1 creates a weaker ligand field at the Fe(II) centers, and more Fe(II) ions are in the HS state. This behavior is consistent with the previous finding that the loss of protic solvent molecules stabilizes the HS state.<sup>37-40</sup> In contrast, more Fe(II) ions are in the LS state after dehydration of complex 2. It is worth mentioning that the loss of aprotic diethyl ether molecules stabilizes LS Fe(II).<sup>15</sup> The different magnetic behavior of complexes 1 and 2 after dehydration is consistent with the presence of different intermolecular interactions.<sup>41</sup>

In conclusion, we have designed new bis(tridentate) Schiff base ligands and successfully prepared three Fe(II) tetranuclear grid complexes. The spin transition of the complexes can be modulated by the inclusion of bulky substituents and different counteranions. Two of the complexes display spin-crossover at close to room temperature. The reversible spin switch can be controlled by the dehydration-hydration process, which is potentially applicable in chemosensors.<sup>38</sup> Further studies of the  $\text{H}_2\text{L}^x$  ligands and analogous Co(II) complexes are in progress. The results of this research will be reported in the future.

## ■ ASSOCIATED CONTENT

### 📄 Supporting Information

Crystallographic data (CIF files) for complexes 1-3, spectroscopic data, experimental procedures, structural diagrams, and additional magnetic data (Figures S1-S13). This material is available free of charge via the Internet at <http://pubs.acs.org>.

## ■ AUTHOR INFORMATION

### ✉ Corresponding Author

kouhz@mail.tsinghua.edu.cn

### Notes

The authors declare no competing financial interest.

## ■ ACKNOWLEDGMENTS

This work was supported by 973 program (2013CB933403) and the National Natural Science Foundation of China (project nos. 91222104 and 21171103).

## ■ REFERENCES

- (1) Létard, J.-F.; Guionneau, P.; Goux-Capes, L. *Top. Curr. Chem.* **2004**, *235*, 221.
- (2) Muñoz, M. C.; Real, J. A. *Coord. Chem. Rev.* **2011**, *255*, 2068.
- (3) Halcrow, M. A. *Polyhedron* **2007**, *26*, 3523.
- (4) Halder, G. J.; Chapman, K. W.; Neville, S. M.; Mobaraki, B.; Murray, K. S.; Létard, J.-F.; Kepert, C. J. *J. Am. Chem. Soc.* **2008**, *130*, 17552.
- (5) Schneider, B.; Demeshko, S.; Dechert, S.; Meyer, F. *Angew. Chem., Int. Ed.* **2010**, *49*, 9274.
- (6) Wu, D.-Y.; Sato, O.; Einaga, Y.; Duan, C.-Y. *Angew. Chem., Int. Ed.* **2009**, *48*, 1475.
- (7) Grunert, C. M.; Reiman, S.; Spiering, H.; Kitchen, J. A.; Brooker, S.; Gütllich, P. *Angew. Chem., Int. Ed.* **2008**, *47*, 2997.
- (8) Goodwin, H. A. *Top. Curr. Chem.* **2004**, *233*, 59.
- (9) García, Y.; Niel, V.; Muñoz, M. C.; Real, J. A. *Top. Curr. Chem.* **2004**, *233*, 229.



- (10) Thompson, J. R.; Archer, R. J.; Hawes, C. S.; Ferguson, A.; Wattiaux, A.; Mathonière, C.; Clérac, R.; Kruger, P. E. *Dalton Trans.* **2012**, *41*, 12720.
- (11) Lennartson, A.; Bond, A. D.; Piligkos, S.; McKenzie, C. J. *Angew. Chem., Int. Ed.* **2012**, *51*, 11049.
- (12) Sheu, C.-F.; Pillet, S.; Lin, Y.-C.; Chen, S.-M.; Hsu, I.-J.; Lecomte, C.; Wang, Y. *Inorg. Chem.* **2008**, *47*, 10866.
- (13) Murray, K. S. *Eur. J. Inorg. Chem.* **2008**, 3101.
- (14) Rajadurai, C.; Qu, Z.; Fuhr, O.; Gopalan, B.; Kruk, R.; Ghafari, M.; Ruben, M. *Dalton Trans.* **2007**, 3531.
- (15) Nihei, M.; Han, L.; Oshio, H. *J. Am. Chem. Soc.* **2007**, *129*, 5312.
- (16) Ruben, M.; Lehn, J.-M.; Vaughan, G. *Chem. Commun.* **2003**, 1338.
- (17) Breuning, E.; Ruben, M.; Lehn, J.-M.; Renz, F.; Garcia, Y.; Ksenofontov, V.; Gütlich, P.; Wegelius, E.; Rissanen, R. *Angew. Chem., Int. Ed.* **2000**, *39*, 2504.
- (18) Newton, G. N.; Onuki, T.; Shiga, T.; Noguchi, M.; Matsumoto, T.; Mathieson, J. S.; Nihei, M.; Nakano, M.; Cronin, L.; Oshio, H. *Angew. Chem., Int. Ed.* **2011**, *50*, 4844.
- (19) Milway, V. A.; Abedin, S. M. T.; Niel, V.; Kelly, T. L.; Dawe, L. N.; Dey, S. K.; Thompson, D. W.; Miller, D. O.; Alam, M. S.; Muller, P.; Thompson, L. K. *Dalton Trans.* **2006**, 2835.
- (20) Onions, S. T.; Frankin, A. M.; Horton, P. N.; Hursthouse, M. B.; Matthews, C. J. *Chem. Commun.* **2003**, 2864.
- (21) Zhao, Y.; Guo, D.; Liu, Y.; He, C.; Duan, C. *Chem. Commun.* **2008**, 5725.
- (22) Zhao, L.; Matthews, C. J.; Thompson, L. K.; Heath, S. L. *Chem. Commun.* **2000**, 265.
- (23) Patroniak, V.; Baxter, Paul, N. W.; Lehn, J.-M.; Kubicki, M.; Nissinen, M.; Rissanen, K. *Eur. J. Inorg. Chem.* **2003**, 4001.
- (24) Dawe, L. N.; Shuvaev, K. V.; Thompson, L. K. *Inorg. Chem.* **2009**, *48*, 3323.
- (25) Li, F.; Clegg, J. K.; Goux-Capes, L.; Chastanet, G.; D'Alessandro, D. M.; Letard, J.-F.; Kepert, C. J. *Angew. Chem., Int. Ed.* **2011**, *50*, 2820.
- (26) Boldog, I.; Munoz-Lara, F. J.; Gaspar, A. B.; Munoz, M. C.; Seredyuk, M.; Real, J. A. *Inorg. Chem.* **2009**, *48*, 3710.
- (27) Wei, R.-J.; Huo, Q.; Tao, J.; Huang, R.-B.; Zheng, L.-S. *Angew. Chem., Int. Ed.* **2011**, *50*, 8940.
- (28) Ruben, M.; Breuning, E.; Lehn, J.-M.; Ksenofontov, V.; Renz, F.; Gütlich, P.; Vaughan, G. B. M. *Chem.—Eur. J.* **2003**, *9*, 4422.
- (29) Nihei, M.; Ui, M.; Yokota, M.; Han, L.; Maeda, A.; Kishida, H.; Okamoto, H.; Oshio, H. *Angew. Chem., Int. Ed.* **2005**, *44*, 6484.
- Mondal, A.; Li, Y.; Herson, P.; Seuleiman, M.; Boillot, M.-L.; Riviere, E.; Julve, M.; Rechignat, L.; Bousseksou, A.; Lescouezec, R. *Chem. Commun.* **2012**, *48*, 5653.
- (30) Stefankiewicz, A. R.; Rogez, G.; Harrowfield, J.; Sobolev, A. N.; Madalan, A.; Huuskonen, J.; Rissanen, K.; Lehn, J.-M. *Dalton Trans.* **2012**, *41*, 13848.
- Stefankiewicz, A. R.; Rogez, G.; Harrowfield, J.; Drillon, M.; Lehn, J.-M. *Dalton Trans.* **2009**, 5787.
- (31) Koningsbruggen, P. J.; Maeda, Y.; Oshio, H. *Top. Curr. Chem.* **2004**, *233*, 259.
- (32) Wang, Y.-T.; Cui, A.-L.; Shen, D.-Z.; Kou, H.-Z. *Polyhedron* **2013**, *52*, 970.
- (33)  $\Sigma$  is the sum of the deviations from 90° of the 12 *cis* N–Fe–N angles in the coordination sphere Guionneau, P.; Marchivie, M.; Bravic, G.; Letard, J.-F.; Chasseau, D. *J. Mater. Chem.* **2002**, *12*, 2546.
- (34)

$$\Delta = \frac{1}{6} \sum_{n=1,6} \left[ \frac{(d_n - \langle d \rangle)}{\langle d \rangle} \right]^2$$

where  $\langle d \rangle$  and  $d_n$  are the mean Fe–N bond length and the six Fe–N bond lengths along six different directions, respectively: Rodriguez-Carvajal, J.; Hennion, M.; Moussa, F.; Moudou, A. H.; Pinsard, L.; Revcolevschi, A. *Phys. Rev.* **1998**, *B57*, R3189.

(35) Shepherd, H. J.; Palamarciuc, T.; Rosa, P.; Guionneau, P.; Molnar, G.; Letard, J.-F.; Bousseksou, A. *Angew. Chem., Int. Ed.* **2012**, *51*, 3910.

(36) Tovee, C. A.; Kilner, C. A.; Barrett, S. A.; Thomas, J. A.; Halcrow, M. A. *Eur. J. Inorg. Chem.* **2010**, 1007.

Genre, C.; Jeanneau, E.; Bousseksou, A.; Luneau, D.; Borshch, S. A.; Matouzenko, G. S. *Chem.—Eur. J.* **2008**, *14*, 697.

(37) Li, B.; Wei, R.-J.; Tao, J.; Huang, R.-B.; Zheng, L.-S.; Zheng, Z. J. *Am. Chem. Soc.* **2010**, *132*, 1558.

Lin, J.-B.; Xue, W.; Wang, B.-Y.; Tao, J.; Zhang, W.-X.; Zhang, J.-P.; Chen, X.-M. *Inorg. Chem.* **2012**, *51*, 9423.

Zhang, W.; Zhao, F.; Liu, T.; Yuan, M.; Wang, Z.-M.; Gao, S. *Inorg. Chem.* **2007**, *46*, 2541.

(38) Halder, G. J.; Kepert, C. J.; Moubaraki, B.; Murray, K. S.; Cashion, J. D. *Science* **2002**, *298*, 1762.

(39) Leita, B. A.; Moubaraki, B.; Murray, K. S.; Smith, J. P. *Polyhedron* **2005**, *24*, 2165.

Niel, V.; Thompson, A. L.; Munoz, M. C.; Galet, A.; Goeta, A. E.; Real, J. A. *Angew. Chem., Int. Ed.* **2003**, *42*, 3760.

Garcia, Y.; van Koningsbruggen, P. J.; Lapouyade, R.; Fournes, L.; Rabardel, L.; Kahn, O.; Ksenofontov, V.; Levchenko, G.; Gütlich, P. *Chem. Mater.* **1998**, *10*, 2426.

Vreugdenhil, W.; van Diemen, J. H.; de Graaff, R. A. G.; Haasnoot, J. G.; Reedijk, J.; van der Kraan, A. M.; Kahn, O.; Zarembowitch, J. *Polyhedron* **1990**, *9*, 2971.

(40) Hayami, S.; Gu, Z.-z.; Yoshiki, H.; Fujishima, A.; Sato, O. *J. Am. Chem. Soc.* **2001**, *123*, 11644.

(41) Gonzalez-Prieto, R.; Fleury, B.; Schramm, F.; Zoppellaro, G.; Chandrasekar, R.; Fuhr, O.; Lebedkin, S.; Kappes, M.; Ruben, M. *Dalton Trans.* **2011**, *40*, 7564.